Phonon-induced electron relaxation in weakly confined single and coupled quantum dots

Juan I. Climente,[1,*] Andrea Bertoni,[1] Guido Goldoni,[1,2] and Elisa Molinari[1,2]

[1]*CNR-INFM S3, Via Campi 213/A, 41100 Modena, Italy*

[2]*Dipartimento di Fisica, Università degli Studi di Modena e Reggio Emilia, Via Campi 213/A, 41100 Modena, Italy*

We investigate charge relaxation rates due to acoustic phonons in weakly confined quantum dot systems, including both deformation potential and piezoelectric field interactions. Single-electron excited states lifetimes are calculated for single and coupled quantum dot structures, both in homonuclear and heteronuclear devices. Piezoelectric field scattering is shown to be the dominant relaxation mechanism in many experimentally relevant situations. On the other hand, we show that appropriate structure design allows to minimize separately deformation potential and piezolectric field interactions, and may bring electron lifetimes in the range of microseconds.

I. INTRODUCTION

Single-electron excited states lifetimes in GaAs-based quantum dots (QDs) are usually limited to the order of nanoseconds.[1,2] This limit is set mainly by acoustic-phonon scattering, which has been shown to be the dominant scattering mechanism between discrete energy states with few-meV gap in both single[1,2] and vertically coupled[3,4] quantum dots (SQDs and CQDs). Prediction of, and control over the electron relaxation rates is desirable for many possible QD applications, ranging from decoherence-free implementation of quantum gates[5] to efficient QD lasers.[6,7] It is also desirable in order to achieve high-resolution optical spectroscopy, since this requires that (nonradiative) phonon scattering rates are smaller than (radiative) photon emission and absorption rates. Therefore, the knowledge of the physics of electron coupling to acoustic phonons in these nanostructures is of great interest.

In a pioneering work, Bockelmann investigated theoretically the influence of lateral (spatial and magnetic) confinement on the single-electron relaxation rates in parabolic QDs.[8] To this end, he considered the deformation potential (DP) coupling between electrons and longitudinal acoustic phonons, while neglecting piezoelectric (PZ) coupling on the grounds of its weaker contribution in two-dimensional (2D) GaAs/Ga_xAl_{1-x}As structures, and the fact that a similar qualitative behavior could be expected in QDs. Using the same assumption, it has been recently proposed that orders-of-magnitude suppression of phonon-induced scattering rates can be achieved[5,9,10] in properly designed CQD structures, and the effect of electron-electron interaction in multielectron QD structures has been investigated.[11]

On the other hand, recent theoretical and experimental works suggest that electron-acoustic phonon scattering due to PZ field interaction is indeed relevant for momentum and spin-relaxation processes in QDs,[2,12] and may even provide the leading contribution to charge decoherence in laterally coupled QDs.[13,14] Therefore, the use of a theoretical model which considers simultaneously both DP and PZ coupling of electrons to acoustic phonons in QDs appears necessary to evaluate quantitatively electron relaxation rates and assess to which extent previous predictions are affected by the PZ field.

In this paper we study the phonon-induced single-electron relaxation rates in realistic models of weakly confined single and vertically coupled QDs, taking into account both DP and PZ mechanisms. The contribution of each relaxation channel is singled out, and the regimes where each coupling mechanism prevails are established. The PZ coupling is shown to be the prevailing one in several experimental situations. Furthermore, we show that QD devices with maximum lifetimes, in the range of microseconds, can be realized not only in coupled QDs, as previously predicted,[5,9] but also in single QDs.

II. THEORETICAL CONSIDERATIONS

The theoretical model we use is essentially the same as our previous works,[9,10] but now we include the scattering rate arising from the PZ field due to longitudinal-acoustic (LA) and transverse-acoustical (TA) phonons. We study GaAs/AlGaAs dots with disk shape and confinement energy in the range of few meV.[1,2,15] The confinement potential has been modeled as a quantum well in the growth direction z, formed by the heterostructure band offset, while in the xy plane a 2D parabolic confinement is assumed, which gives rise to the Fock-Darwin level structure.[16] The three-dimensional single-particle electronic states are computed within the envelope function approximation. The electron states are labelled by the three quantum numbers (n,m,g), where $n=0,1,2,\dots$ denotes the nth state with azimuthal angular momentum $m=0,\pm 1,\pm 2,\dots$ and parity g. Here g $=0$ (1) stands for even (odd) parity with respect to the reflection about the $z=0$ plane. We consider bulk phonons with linear dispersion $\omega_{\sigma q}=c_\sigma|\mathbf{q}|$, where c_σ is the sound velocity of LA ($\sigma=$LA) or TA ($\sigma=$TA) phonon modes in the QD material, and $\mathbf{q}$ is the momentum.[17] The electron-phonon interaction Hamiltonian reads $\mathcal{H}_{e-p}=\sum_{\nu\mathbf{q}}M_\nu(\mathbf{q})(b_\mathbf{q}e^{i\mathbf{qr}}+b_\mathbf{q}^\dagger e^{-i\mathbf{qr}})$, where $b_\mathbf{q}$ and $b_\mathbf{q}^\dagger$ are the phonon annihilation and creation operators, respectively, and $M_\nu(\mathbf{q})$ is the scattering matrix element corresponding to the electron scattering mechanism ν (see below). For simplicity we assume zero temperature, so that phonon absorption and multiphonon processes are negligible. The relaxation rate between the ini-

tial (occupied) state $|\Psi_i\rangle$ and the final (unoccupied) state $|\Psi_f\rangle$ is determined by the Fermi golden rule,

$$\tau_{if}^{-1} = \frac{2\pi}{\hbar} \sum_{\nu\mathbf{q}} |M_\nu(\mathbf{q})|^2 |\langle\Psi_f|e^{-i\mathbf{q}\mathbf{r}}|\Psi_i\rangle|^2 \delta(|E_f - E_i| - E_q), \tag{1}$$

where E_f and E_i stand for the final and initial electron states energy and $E_q = \hbar\omega_{\sigma q}$ represents the phonon energy. It is clear from the above equation that the relaxation is mediated by phonons whose energy matches that of the transition between the initial and final electron states. The electron-phonon scattering for a zinc-blende crystal is composed of the following contributions:[12,18,19]

(i) The electron-LA phonon scattering due to the deformation potential (ν=LA-DP),

$$|M_{\text{LA-DP}}(\mathbf{q})|^2 = \frac{\hbar D^2}{2dc_{\text{LA}}\Omega}|\mathbf{q}|; \tag{2}$$

(ii) the electron-LA phonon scattering due to the PZ field (ν=LA-PZ),

$$|M_{\text{LA-PZ}}(\mathbf{q})|^2 = \frac{32\pi^2\hbar\, e^2 h_{14}^2}{\epsilon^2 dc_{\text{LA}}\Omega} \frac{(3q_x q_y q_z)^2}{|\mathbf{q}|^7}; \tag{3}$$

(iii) the electron-TA phonon scattering due to the PZ field (ν=TA-PZ),

$$|M_{\text{TA-PZ}}(\mathbf{q})|^2 = \frac{32\pi^2\hbar\, e^2 h_{14}^2}{\epsilon^2 dc_{\text{TA}}\Omega} \times \left| \frac{q_x^2 q_y^2 + q_y^2 q_z^2 + q_z^2 q_x^2}{|\mathbf{q}|^5} - \frac{(3q_x q_y q_z)^2}{|\mathbf{q}|^7} \right|. \tag{4}$$

In the above expressions D, d, and Ω stand for the crystal acoustic deformation potential constant, density, and volume, respectively. e is the electron charge, h_{14} is the PZ constant, and ϵ is the static dielectric constant. Note that the sum in Eq. (1) runs twice over ν=TA-PZ, to account for the two transverse phonon modes (both identical under the Ref. 19 approximation for zinc-blende crystals). For the analysis of the results presented in the following sections, it is useful to realize that differences between the various scattering mechanisms in Eq. (1) arise from (i) the diverse matrix elements $M_\nu(\mathbf{q})$; (ii) the different value of $\mathbf{q}$ associated with a given transition energy for TA and LA phonons which enters $|\langle\Psi_f|e^{-i\mathbf{q}\mathbf{r}}|\Psi_i\rangle|^2$. The former factor introduces some qualitative differences in the behavior, whereas the latter mostly shifts the transition energy values at which LA- and TA-phonon scattering with the same phonon momentum occur.

In this work we consider mostly relaxation rates from the first excited to the ground electron state in SQDs and CQDs. This is often the most relevant transition, since many QD applications rely on the formation of two-level systems, and it can be monitored, e.g., by means of pump-and-probe techniques.[1,2] Assuming Fock-Darwin level structure, for SQDs this corresponds to a transition from a p (m=1) to a s (m=0) level. For CQDs this corresponds to the isospin transition from an antisymmetric (g=1) to a symmetric (g=0) state. The behavior of transition rates from higher excited
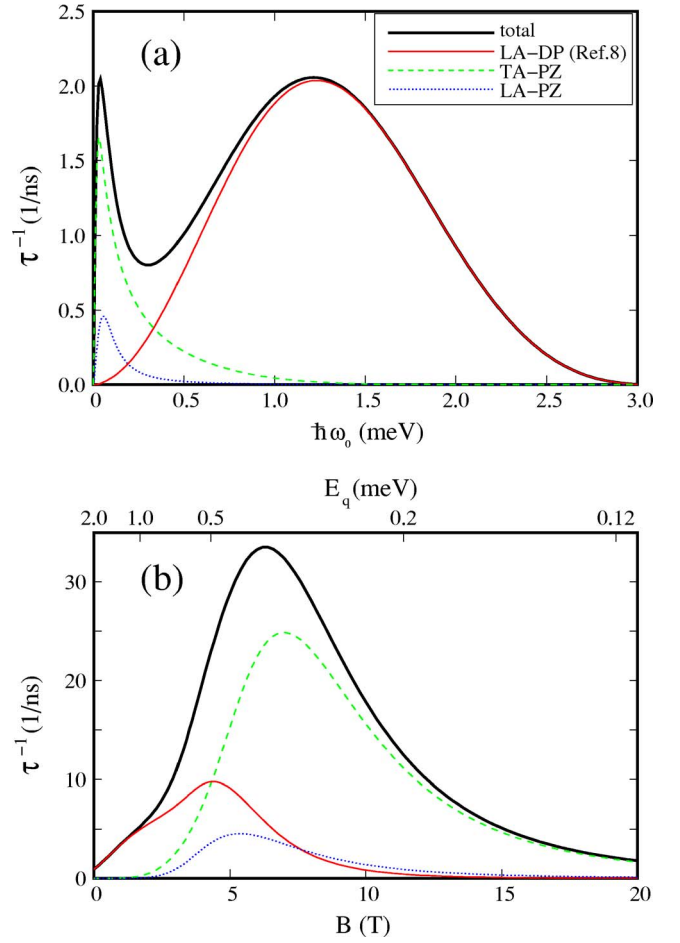

FIG. 1. (Color online) Acoustic phonon scattering rate as a function of (a) lateral confinement, and (b) magnetic field, for the electron transition $(n,m,g)=(0,1,0)\rightarrow(0,0,0)$ in a GaAs/Al$_{0.3}$Ga$_{0.7}$As QD with L_z=10 nm. In panel (b) $\hbar\omega_0$=2 meV, and the upper scale shows the emitted phonon energy E_q.

states is qualitatively similar, except for the presence of a larger number of decay channels which smears the features of direct scattering between two selected states.[8] We use GaAs/Al$_{0.3}$Ga$_{0.7}$As material parameters:[20] electron effective mass m^*=0.067, band-offset V_c=243 meV, d=5310 kg/m^3, D=8.6 eV, ϵ=12.9, and h_{14}=1.41$\times$10^9 V/m. For the sound speed c_σ, we take into account that in cylindrical QDs most of the scattering arises from phonon propagation close to the growth direction.[10] We then assume that the QDs are grown along the [1 0 0] direction and use the corresponding values c_{LA}=4.72$\times$10^3 m/s and c_{TA}=3.34$\times$10^3 m/s.[21]

III. RELAXATION IN SINGLE QUANTUM DOTS

In this section we study the $(n,m,g)=(0,1,0)\rightarrow(0,0,0)$ transition in SQDs as a function of the spatial and magnetic confinement.

Figure 1(a) illustrates the scattering rate of a SQD with well width L_z=10 nm as a function of the harmonic confinement energy, $\hbar\omega_0$. For most lateral confinements, DP coupling (the only source of relaxation considered in Ref. 8)

gives the largest contribution. However, for weak confinements ($\hbar\omega_0 < 0.4$ meV) PZ coupling prevails, so that the total scattering rate shows two maxima instead of one. This is because the different wave vector dependence in the DP and PZ matrix elements ($\sqrt{q}$ for DP versus $1/\sqrt{q}$ for PZ interaction) yields maxima at different confinement energies (i.e., different energies of the emitted phonons). Moreover, we observe that the PZ contribution coming from TA phonons is larger than that of LA phonons. This holds for almost all calculations throughout this paper. Although the shape of PZ scattering rate is different from the DP one, the limiting behavior is similar: it tends to zero at very weak confinement potentials because of the decreasing phonon density of states; it also tends to zero in the strong confinement limit, due to the orthogonality of the electron states which makes the factor $\langle \Psi_f | e^{-i\mathbf{q}\mathbf{r}} | \Psi_i \rangle$ vanish rapidly when the phonon wavelength λ_q is shorter than the lateral (i.e., the largest) confinement length.[8,10]

The lateral confinement and transition energy in a QD can be also modulated by a magnetic field (B) applied along the growth direction. In Fig. 1(b) we show the B dependence of the scattering rate for a SQD with $L_z = 10$ nm and $\hbar\omega_0 = 2$ meV. We note that the PZ rate is negligible at zero magnetic field, but it rapidly increases with B and soon exceeds the DP rate. This is because the energy of the (0,1,0) and (0,0,0) states converge with increasing B,[16] so that the energy of the emitted phonon becomes ever smaller (see upper scale in the figure) and the PZ matrix elements are maximized. As a consequence, the maximum of the total scattering rate, including the PZ interaction, is over three times higher than the one calculated including only the DP mechanism; this difference is even larger for dots with weaker lateral confinement (not shown). Therefore, the inclusion of PZ interactions to properly describe the scattering rate in SQDs in the presence of magnetic fields is critical. This result also justifies recent findings reported by other authors, which claim that spin relaxation rate is mostly determined by TA-PZ scattering:[12] spin-orbit mixing is only significant when B drives the electron states involved close in energy,[22] and then TA-PZ is by far the most important source of phonon scattering. One may note in Fig. 1(b) that the maxima of TA-PZ and LA-PZ scattering rates take place at different values of B, in spite of the fact that the matrix elements of both mechanisms depend on the phonon wave vector as $1/\sqrt{q}$. This is because of the different sound velocities of TA and LA phonon modes, which associate the same phonon energy with different wave vectors, $|\mathbf{q}| = E_q/(\hbar c_\sigma)$.

IV. CONTROLLING ELECTRON RELAXATION

A. Single quantum dots

Electron-acoustic phonon interaction in SQDs is to a large extent determined by the interplay of lateral confinement length, quantum well width, and phonon wavelength.[8] However, in weakly confined QDs vertical confinement is usually much stronger than lateral confinement. As a result, the energy of the transition $(0,1,0) \rightarrow (0,0,0)$ (and thus the wavelength of the emitted phonon) is exclusively determined by
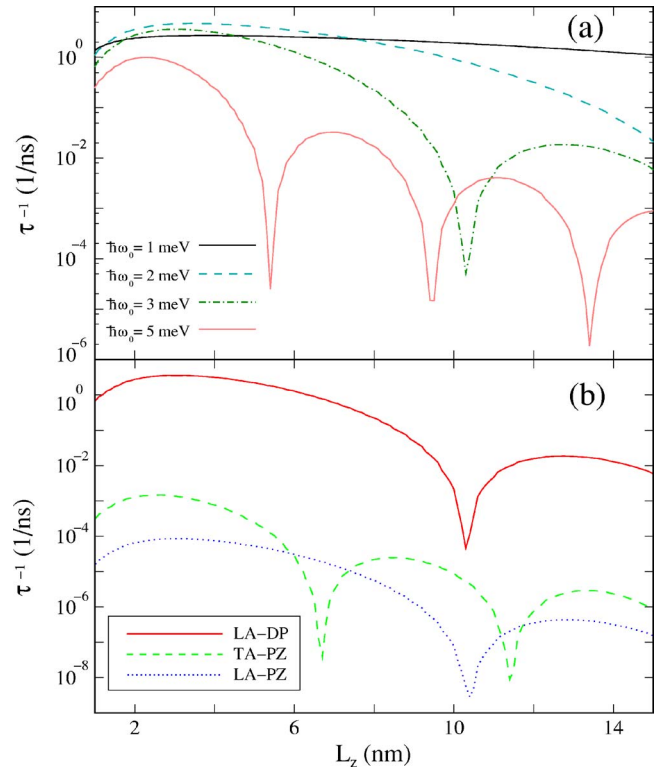

FIG. 2. (Color online) (a) Acoustic phonon total scattering rate as a function of the quantum well width, L_z for the electron transition $(n,m,g) = (0,1,0) \rightarrow (0,0,0)$ in a SQD, at selected values of lateral confinement $\hbar\omega_0$. (b) Individual contributions from each scattering mechanism in a QD with $\hbar\omega_0 = 3$ meV.

the lateral confinement. Therefore, if we fix the lateral confinement and change only the well width we could expect that the scattering rate exhibits periodic oscillations, with maxima when $L_z \simeq (j+1/2)\lambda_q$ (i.e., the electron wave function along the quantum well direction is in-phase with the phonon wave) and minima when $L_z \simeq j\lambda_q$ (i.e., the electron wave function is in antiphase with the phonon wave). We explore this possibility in Fig. 2(a), where the effect of vertical confinement on the total scattering rates of SQDs with different $\hbar\omega_0$ is illustrated. For $\hbar\omega_0 = 1$ and $\hbar\omega_0 = 2$ meV no scattering minima are observed, indicating that λ_q is still too large for the range of L_z shown (which are indeed typical well widths of realistic devices). However, for $\hbar\omega_0 = 3$ meV we observe a striking dip at about $L_z = 10.5$ nm, where the scattering rate is suppressed by orders of magnitude due to the antiphase relation between the electron wave function and the phonon plane wave. For $\hbar\omega_0 = 5$ meV order-of-magnitude damping of the scattering rate at several well widths values is observed. A similar geometry-induced suppression of the scattering rate was previously proposed for CQDs,[5] but here we show that it is also feasible for SQDs with realistic dimensions if the confinement energy is in the proper range. This result may be of great significance for quantum coherence preservation in SQD devices.

Figure 2(b) depicts separately the LA-DP, TA-PZ, and LA-PZ scattering rates in the SQD with $\hbar\omega_0 = 3$ meV. One can see that, in the absence of external fields, LA-DP scattering rate constitutes the dominant relaxation mechanism by
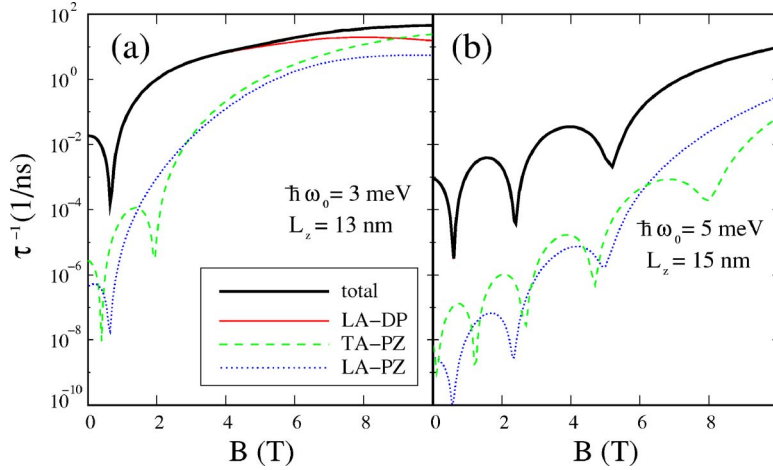
FIG. 3. (Color online) Acoustic phonon scattering rate as a function of the magnetic field for the electron transition $(n,m,g)=(0,1,0) \rightarrow (0,0,0)$ in selected SQDs.

at least one order of magnitude. This accounts for the fact that only one damping dip is observed in the total scattering rate, even though TA-PZ scattering shows two dips due to the smaller speed of TA phonons.

From a practical point of view, it is clearly difficult to fabricate QDs with the exact aspect ratio (i.e., lateral vs vertical confinement) which meets the scattering rate minima plotted in Fig. 2. Therefore, we next show that the damping of phonon-induced relaxation rate in SQDs can also be achieved by means of external magnetic fields. Let us consider a SQD of lateral confinement $\hbar\omega_0$ and well width $L_z > L_z^{crit}$, where L_z^{crit} is a well width value leading to a scattering rate minimum. A magnetic field applied along the growth direction decreases the energy spacing between the $(0,1,0)$ and $(0,0,0)$ states and, as a consequence, increases the wavelength of the emitted phonon. It is then possible to tune B in order to obtain the phonon wavelength which is in antiphase with the electron wave function in the quantum well of width L_z. This is illustrated in Fig. 3(a) for a SQD with $\hbar\omega_0=3$ meV and $L_z=13$ nm, and in Fig. 3(b) for a SQD with $\hbar\omega_0=5$ meV and $L_z=15$ nm. In both cases scattering rate dips similar to those observed in Fig. 2 are forced by the magnetic field. Moreover, the total scattering rate suppressions are again well described in terms of DP coupling, since PZ coupling becomes significant at larger values of B only. This indicates that, as a general rule, for usual QD heights, phonon energies leading to scattering rate suppression derive from lateral (spatial or magnetic) confinements which are strong enough to disregard PZ interaction.

B. Vertically coupled quantum dots

CQDs constitute an interesting system for phonon scattering modulation because they allow the electron charge to distribute among the various quantum wells along the vertical direction. As a consequence, the total height of the artificial molecule, as CQDs are often called, replaces the SQD height as the critical parameter leading to relaxation rate suppressions when it is in antiphase with the phonon wavelength. It is then possible to minimize the scattering rate of the $(0,1,0) \rightarrow (0,0,0)$ (intradot) transition by proper structure design[5] or using magnetic fields[9,10] even when the lateral confinement is so weak that the suppression described above

for SQDs cannot occur. In particular, it has been predicted that for periodic values of the interdot barrier thickness, L_b, decoherence-free systems may be built.[5] This prediction was obtained considering only DP scattering, and one may wonder whether this picture holds when we include PZ interactions. To this end, in Fig. 4 we plot the scattering rate of two CQDs with $L_z=5$ nm and $\hbar\omega_0=1$ meV, as a function of the barrier thickness. The total scattering rate oscillates periodically, with most of the contribution coming from DP interactions.[23] Nevertheless, the TA-PZ contribution becomes predominant at the values of L_b where complete suppression of LA-DP scattering is predicted (see insets around $L_b=5$ nm and $L_b=25$ nm in Fig. 4); indeed, the DP and PZ mechanism have minima at different L_b due to the difference in the sound velocity and, therefore, in the wavelength of the emitted phonons. This imposes a limit on the barrier-thickness-induced suppression of intradot transition rates reported in Ref. 5, which can be nonetheless minimized by growing CQDs with stronger lateral confinement, so that PZ interaction strength rapidly decreases (see Fig. 1).

Recently we have shown that B-induced control of the DP scattering rate in CQDs is also possible.[9,10] Again, the ques-
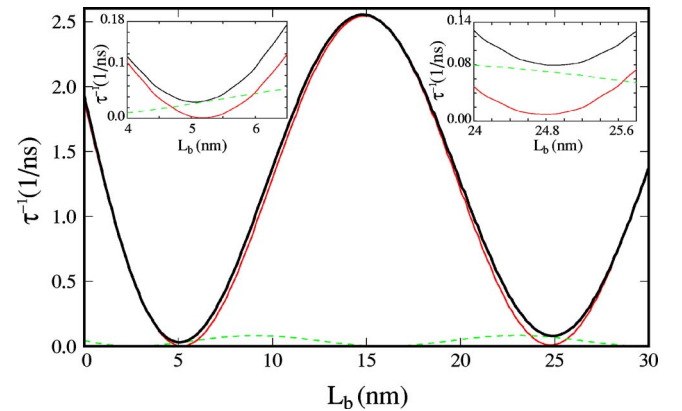

FIG. 4. (Color online) Acoustic phonon scattering rate as a function of the barrier width L_b for the electron transition $(n,m,g)=(0,1,0) \rightarrow (0,0,0)$ in a CQD structure with $\hbar\omega_0=1$ meV and $L_z=5$ nm. The insets zoom in the regions around the DP scattering minima. Scattering mechanisms are represented as in the legend of Fig. 1.
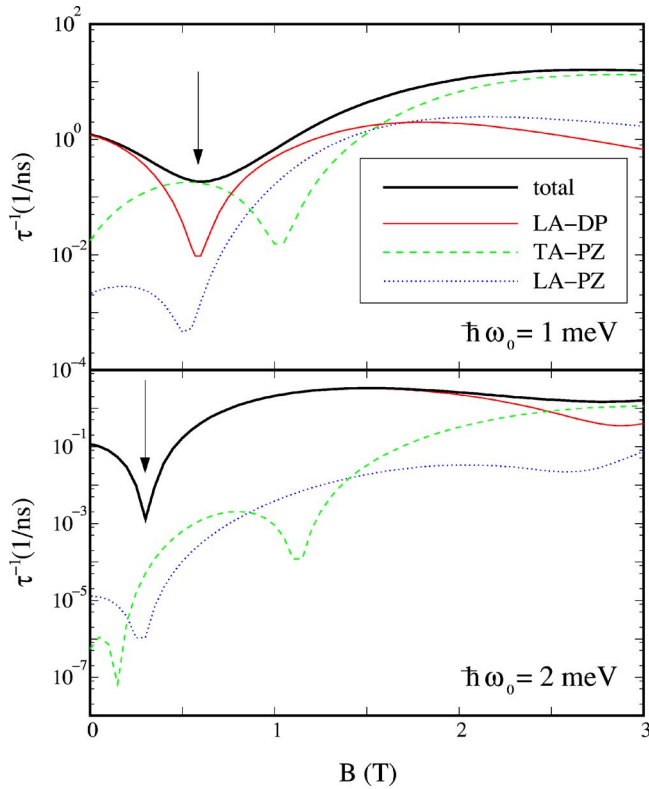
FIG. 5. (Color online) Acoustic phonon scattering rate as a function of the magnetic field for the electron transition $(n,m,g)=(0,1,0)\rightarrow(0,0,0)$ in two CQD structures with $L_z=12$ nm, $L_b=5$ nm, and different lateral confinement. The arrows point to the position of the relaxation rate minima expected including the DP interaction only (Refs. 9 and 10).

tion arises concerning the influence of PZ scattering in this picture. Figure 5 illustrates the relaxation rate for two CQD structures with $L_z=12$ nm, $L_b=5$ nm, and different lateral confinement. The arrows point to the position of the expected minima according to the DP description.[9,10] One can see that for $\hbar\omega_0=1$ meV the minimum of DP scattering coincides with the maximum of TA-PZ scattering, and therefore the expected suppression of the relaxation rate is greatly inhibited. Yet, this no longer occurs for $\hbar\omega_0=2$ meV, where PZ interactions are less relevant at weak fields due to the stronger spatial lateral confinement. It is worth stressing that this suppression is found for a lateral confinement strength which is too weak for the SQD-based suppression to be efficient [see $\hbar\omega_0=2$ meV curve in Fig. 2(a)]. On the other hand, simultaneous control of DP and TA-PZ scattering rates, aimed at making their respective minima coincide, is an intricate process which follows from the interplay among QD geometry, composition, and growth direction. Therefore, we conclude that CQDs stand as a firm alternative to SQDs for control of intradot transitions phonon relaxation only when both scattering sources have significantly different weights. This can be achieved for instance using QDs with lateral confinement ~ 2 meV, or building QDs with narrow-gap materials where the spacing between conduction band states is increased and hence PZ influence is smaller.

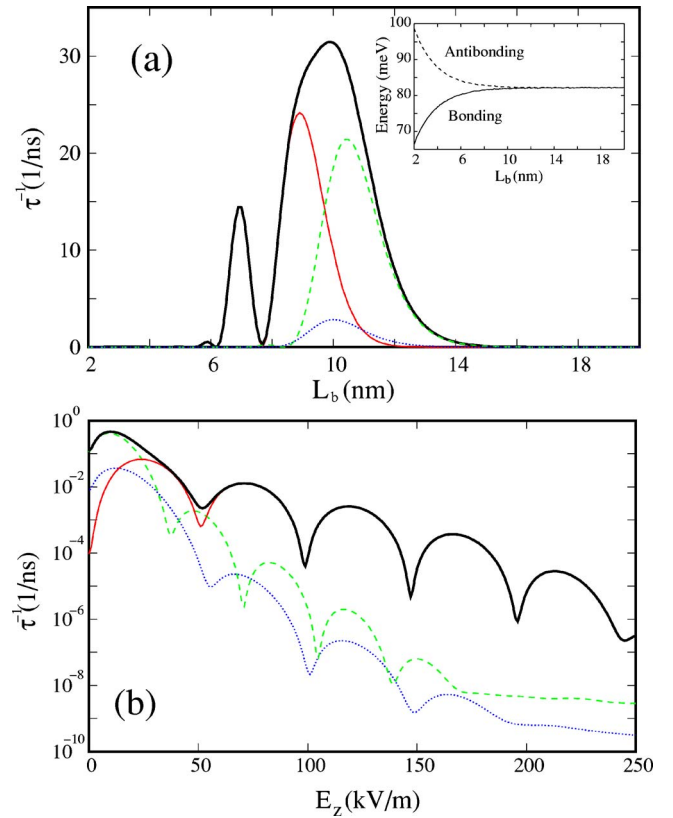Next, we analyze the transition rate between the lowest bonding and antibonding states of two CQDs (n,m,g)

FIG. 6. (Color online) Acoustic phonon scattering rate as a function of (a) the barrier width L_b, and (b) the electric field, for the electron transition $(n,m,g)=(0,0,1)\rightarrow(0,0,0)$ in a CQD structure with $\hbar\omega_0=5$ meV and $L_z=5$ nm. Inset of panel (a), energy of the lowest bonding (solid line) and antibonding (dashed line) states vs barrier width. In panel (b) $L_b=15$ nm. Scattering mechanisms are represented as in the legend of Fig. 1.

$=(0,0,1)\rightarrow(0,0,0)$ (interdot or isospin transition). The interest of this transition is in part connected with the demand of coherent tunneling between the two dots for isospin-based implementations of quantum gates,[24] as well as with quantum dot cascade laser devices performance.[7] The wavelength of the emitted phonon is in this case controlled by the tunneling energy, which can be tuned by means of either the barrier thickness or an electric field applied along the z direction (E_z).[9] In Fig. 6 we study the effect of both mechanisms for CQD devices with $L_z=5$ nm and $\hbar\omega_0=5$ meV. Figure 6(a) represents the transition rate vs the barrier width. The total rate depends strongly on L_b. However, only a few nonperiodic oscillations are observed, as opposed to the intradot transition case (Fig. 4). This is due to the changing tunneling energy (see inset), which makes the phonon wavelength vary exponentially with L_b. On the other hand, we note that PZ interactions become dominant when the barrier thickness is large, owing to the small tunneling energy. These results can be related to recent experiments which reported different relative photoluminescence intensities for bonding and antibonding exciton states in a pair of CQDs as a function of the interdot distance.[4] Since the intensity of photoluminescence peaks is proportional to the lifetime of conduction states, and acoustic phonon coupling was identified as

the main relaxation source in the experiment, these observations indicated a nonmonotonic dependence of the antibonding state lifetime on the barrier thickness, in agreement with Fig. 6(a). In Fig. 6(b) we depict the E_z-dependent scattering rate corresponding to CQDs with $L_b = 15$ nm. As in previous works,[9] we find order-of-magnitude oscillations of the DP scattering rate, which also take place for PZ rates albeit with different period for the TA phonons. Interestingly, the PZ scattering rate decay is much faster than that of the DP, due to the different wave-vector dependence of the matrix element. As a result, even if PZ prevails in the absence of external fields, the use of an electric field soon turns DP into the dominant relaxation mechanism, and one can think of electric-field-induced suppressions of the scattering rate in terms of DP interaction only. We would like to point out that the interdot transition rate minima observed in Fig. 6 have no counterpart in laterally coupled dots.[14] This represents a fair advantage of vertically coupled structures with regard to quantum gate implementation schemes, since it allows one to reduce charge decoherence times dramatically. The underlying reason for this difference lies in the larger total vertical dimension of the vertically coupled double QD system, which makes it possible to reach antiphase relation between the electron wave function and the phonon plane wave along z for small tunneling energies (i.e., long phonon wavelengths). Since only electron-phonon coupling along the growth direction (not in the in-plane direction) are responsible for scattering rate oscillations (see, e.g., Fig. 3 of Ref. 10), and laterally coupled dots are usually low, no scattering reduction is expected in such structures.

So far we have considered CQDs composed by two identical dots (in analogy with atomic molecules, we refer to these systems as homonuclear). However, in practice this is hard to achieve and the size of the coupled dots is usually slightly different, leading to heteronuclear systems.[25,26] Molecular levels are very sensitive to small changes in the size of the coupled dots,[25,27] so that one may also expect significant effects on the transition rates. To analyze this case, in Fig. 7 we consider a CQD structure with $L_b = 10$ nm. Both QDs have the same lateral confinement $\hbar\omega_0 = 5$ meV, but the bottom well width is $L_z = 5$ nm, while the upper well one is $L_z = 5.5$ nm. The effect of an electric field on this heteronuclear system is to introduce order-of-magnitude oscillations which first lead to an enhancement of the scattering rate and then to a reduction in a clearly symmetric fashion. These results are interpreted as follows. In the absence of external fields, bonding and antibonding states (solid and dotted lines in the insets, respectively) localize in opposite wells. As a consequence, the factor $\langle \Psi_f | e^{-i\mathbf{qr}} | \Psi_i \rangle$ in Eq. (1) is reduced as compared to the homonuclear case, where the charge density of bonding and antibonding states are equally distributed between the dots. For a given electric field we can compensate for the different well width of the two QDs, and force an identical charge density distribution of bonding and antibonding states. This maximizes $\langle \Psi_f | e^{-i\mathbf{qr}} | \Psi_i \rangle$ and therefore the relaxation rate. Finally, for stronger fields the original localization of states is reversed. It is also worth noting that the total scattering rate in Fig. 7 is essentially given by the DP interaction, except in the vicinity of the homonuclearity point, where the energy of bonding and antibonding levels
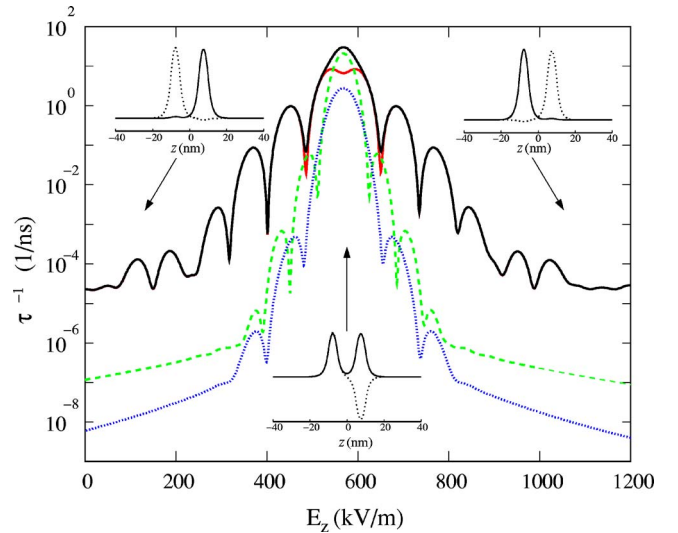

FIG. 7. (Color online) Acoustic phonon scattering rate as a function of the electric field for the electron transition $(n,m,g) = (0,0,1) \rightarrow (0,0,0)$ in a heteronuclear CQD structure, with $L_b = 10$ nm, $\hbar\omega_0 = 5$ mev, $L_z = 5$ nm (bottom QD) and $L_z = 5.5$ nm (upper QD). Insets, electron wave function (arbitrary units) in the double quantum well for $E_z = 0$ kV/cm (left), $E_z = 568$ kV/m (center) and $E_z = 1200$ kV/m (right), with solid (dotted) lines representing the lowest bonding (antibonding) state. Scattering mechanisms are represented as in the legend of Fig. 1.

are very close and TA-PZ relaxation prevails. For practical purposes, one is often interested in obtaining coherent delocalization of the particles between the two dots, i.e., reaching a homonuclear system with long electron lifetimes.[24] Figure 7 shows that a relatively small departure from the electric field which gives the homonuclear charge distribution, from $E_z = 570$ to $E_z = 485$ kV/m, increases the electron lifetime by three orders of magnitude, while partially preserving electron delocalization.

V. SUMMARY

Single-electron relaxation rates in GaAs SQDs and CQDs due to coupling with acoustic phonons have been investigated. PZ interactions due to TA phonons, often disregarded in the literature, constitute the major source of scattering for small (<0.5 meV) electron transition energies. For larger gaps, DP interactions due to LA phonons prevail. Indeed, we identify many situations where PZ effects become critical, such as SQDs subjected to an axial magnetic field or the isospin transition in CQDs with large interdot distances. Nevertheless, we have shown that proper structure design makes it possible to control the scattering rates of both SQDs and CQDs by orders of magnitude. Suppression of the scattering rate in SQDs can be attained for moderately large (few meV) lateral confinement, while CQD structures permit to extend it down to fairly weak lateral confinements. Similar results can be achieved using external fields even when the structures do not have the optimum geometry. Unlike laterally CQDs, vertically CQDs can be used to obtain enhanced electron lifetimes (in the range of microseconds) in excited molecular states, which has important implications for quan-

*Electronic address: climente@unimo.it; URL: http://www.nanoscience.unimo.it/

[1] T. Fujisawa, D. G. Austing, Y. Tokura, Y. Hirayama, and S. Tarucha, Nature (London) **419**, 278 (2002).

[2] T. Fujisawa, D. G. Austing, Y. Tokura, Y. Hirayama, and S. Tarucha, J. Phys.: Condens. Matter **15**, R1395 (2003).

[3] S. Tarucha, T. Fujisawa, K. Ono, D. G. Austing, T. H. Oosterkamp, W. G. van der Wiel, and L. P. Kouwenhoven, Microelectron. Eng. **47**, 101 (1999).

[4] G. Ortner, R. Oulton, H. Kurtze, M. Schwab, D. R. Yakovlev, M. Bayer, S. Fafard, Z. Wasilewski, and P. Hawrylak, Phys. Rev. B **72**, 165353 (2005).

[5] P. Zanardi and F. Rossi, Phys. Rev. Lett. **81**, 4752 (1998); Phys. Rev. B **59**, 8170 (1999).

[6] M. Sugawara, K. Mukai, and H. Shoji, Appl. Phys. Lett. **71**, 2791 (1997).

[7] N. S. Wingreen and C. A. Stafford, IEEE J. Quantum Electron. **33**, 1170 (1997).

[8] U. Bockelmann, Phys. Rev. B **50**, 17271 (1994).

[9] A. Bertoni, M. Rontani, G. Goldoni, F. Troiani, and E. Molinari, Appl. Phys. Lett. **85**, 4729 (2004).

[10] A. Bertoni, M. Rontani, G. Goldoni, F. Troiani, and E. Molinari, Physica E (Amsterdam) **26**, 427 (2005).

[11] A. Bertoni, M. Rontani, G. Goldoni, and E. Molinari, Phys. Rev. Lett. **95**, 066806 (2005).

[12] J. L. Cheng, M. W. Wu, and C. Lü, Phys. Rev. B **69**, 115318 (2004).

[13] Z. J. Wu, K. D. Zhu, X. Z. Yuan, Y. W. Jiang, and H. Zheng, Phys. Rev. B **71**, 205323 (2005).

[14] V. N. Stavrou and X. Hu, Phys. Rev. B **72**, 075362 (2005).

[15] S. Tarucha, D. G. Austing, S. Sasaki, Y. Tokura, W. van der Wiel, and L. P. Kouwenhoven, Appl. Phys. A: Mater. Sci. Process. **71**, 367 (2000); U. Bockelmann, Ph. Roussignol, A. Filoramo, W. Heller, G. Abstreiter, K. Brunner, G. Böhm, and G. Weimann, Phys. Rev. Lett. **76**, 3622 (1996); J. Kyriakidis, M. Pioro-Ladriere, M. Ciorga, A. S. Sachrajda, and P. Hawrylak, Phys. Rev. B **66**, 035320 (2002).

[16] S. M. Reimann and M. Manninen, Rev. Mod. Phys. **74**, 1283 (2002).

[17] The use of bulk phonons has been shown to provide an accurate description of relaxation processes in realistic GaAs/Al$_{1-x}$Ga$_x$As QD samples, see Refs. 1 and 2. However, if the heterostructure materials had significantly different lattice constants or semiconductor surfaces were present close to the dots, confined acoustic phonon modes should be considered, see, e.g., A. A. Balandin, J. Nanosci. Nanotechnol. **5**, 1015 (2005), and references therein.

[18] V. F. Gantmakher and Y. B. Levinson, *Carrier Scattering in Metals and Semiconductors*, Modern Problems in Condensed Matter Sciences, Vol. 19 (Elsevier Science, New York, 1987), Chap. 3.

[19] Averaging over the piezoelectric modulus components to preserve cubic symmetry has been done following J. D. Zook, Phys. Rev. **136**, A869 (1964).

[20] *Physics of Hot Electron Transport in Semiconductors*, edited by C. S. Ting (World Scientific, Singapore, 1992).

[21] *Landolt-Börnstein, Numerical Data and Functional Relationships in Science and Technology, Vol. 17 Semiconductors, Group IV Elements and III-V Compounds*, edited by O. Madelung (Springer-Verlag, Berlin, 1982).

[22] M. Florescu, S. Dickman, M. Ciorga, A. Sachrajda, and P. Hawrylak, Physica E (Amsterdam) **22**, 414 (2004); M. Florescu and P. Hawrylak, Phys. Rev. B **73**, 045304 (2006).

[23] Periodic oscillations of the scattering rate as a function of the interdot barrier thickness are limited in practice by the difficulty of achieving coherent delocalization of the electron charge between the dots when the barrier is too thick. Here we do not consider this effect, and simply show the ideal behavior. Coherent delocalization has been demonstrated in VCQDs up to L_b =8 nm (Ref. 4).

[24] M. Bayer, P. Hawrylak, K. Hinzer, S. Fafard, M. Korkusinski, Z. R. Wasilewski, O. Stern, and A. Forchel, Science **291**, 451 (2001).

[25] M. Pi, A. Emperador, M. Barranco, F. Garcias, K. Muraki, S. Tarucha, and D. G. Austing, Phys. Rev. Lett. **87**, 066801 (2001).

[26] N. N. Ledentsov, V. A. Shchukin, M. Grundmann, N. Kirstaedter, J. Böhrer, O. Schmidt, D. Bimberg, V. M. Ustinov, A. Yu. Egorov, A. E. Zhukov, P. S. Kop'ev, S. V. Zaitsev, N. Yu. Gordeev, Zh. I. Alferov, A. I. Borovkov, A. O. Kosogov, S. S. Ruvimov, P. Werner, U. Gösele, and J. Heydenreich, Phys. Rev. B **54**, 8743 (1996).

[27] L. R. C. Fonseca, J. L. Jimenez, and J. P. Leburton, Phys. Rev. B **58**, 9955 (1998).